Shell structures with ''magic numbers'' of spheres in a swirled dish

Karsten Kötter*
Max-Planck-Institut für Molekulare Physiologie, Postfach 500247, 44202 Dortmund, Germany

Eric Goles†
Departamento de Ingeniería Matemática, FCFM, Universidad de Chile, Casilla 170–3, Santiago, Chile

Mario Markus‡
Max-Planck-Institut für Molekulare Physiologie, Postfach 500247, 44202 Dortmund, Germany
(Received 16 November 1998; revised manuscript received 19 March 1999)

Molecular dynamic simulations of a low number $N \leqslant 54$ of spheres in a swirled dish yield solidlike shell structures with stable rings. In contrast to known granular media, solidification occurs only at singular values of N: 7, 8, 12, 14, 19, 21, 30, 37, 40. Otherwise, we obtain intermittent switching of particles between rings — the average switching time scaling exponentially with a control parameter — or fluidlike disorder. Stable shell structures can be classified by particular geometrical arrangements (one-centered hexagonal, one-centered ''quasicircular,'' three centered, and four centered). [S1063-651X(99)08112-X]

PACS number(s): 68.35.Rh, 02.70.Ns, 47.54.+r

I. INTRODUCTION

Increasing attention is being paid to the ubiquitous but poorly understood granular materials (for reviews, see [1–3]). Technical knowledge about them is important for the control of mixing, unmixing, release from storage, and transport of goods ranging from powders and pills to cereals and gravel. Also, they are relevant to geological processes and astrophysics [3]. Furthermore, they are a challenge to physicists since ordinary hydrodynamics and thermodynamics do not work because of inelastic collisions and the failure of the ergodic hypothesis (see [4] and references therein). A number of unique phenomena occuring in granular materials have been reported; examples are localized states in vertically vibrated layers [5], finger patterns in flows [6], and size segregation [7,8]. While some authors regard granular media as an additional state of matter in its own right, others regard it as a hybrid state of liquid, solid, and gas. A fruitful attitude has been to consider solid-fluid-like transitions [9–11] or stagnant solidlike zones in liquid environments [8,12,13]. In the present work, we shall also consider analogies to fluid and solid phases, including intermediate states.

In order to explore the variety of behavior of particles in a swirled dish, we did computer simulations by using molecular dynamics. In the literature, reasonable computer times and mechanistic simplifications permit us to consider a number N of particles up to 10^4–10^6. In our work, however, we shall deal with a very small number of particles: $5 \leqslant N \leqslant 54$. Such numbers are attractive for the following reasons: (i) Mechanistic simplifications at large N for coping with computational limitations can be avoided; (ii) there is no need for assuming a smaller N than in experiments; (iii) one can explore the sensitive dependence on N, i.e., significant changes for $\Delta N = \pm 1$; (iv) one can deal with situations occuring in real biological systems, as, for example, spherical algae cells ($4 \leqslant N \leqslant 128$), swarming and aggregating within a vesicle [14]. For N in this small range, simulations of the following systems have been reported: (i) Beads in one dimensional (1D) vibrating columns [15]; and (ii) disks in two-dimensional (2D) swirled dishes displaying a transition from rotation in swirling direction to a ''reptation'' in the opposite direction [16].

II. METHODS

In this work we perform three-dimensional (3D) simulations of N spheres with radii $r_p = 5$ mm and density $\rho = 2.5\ \mathrm{g\,cm^{-3}}$. A particle i is described by its position $\vec{r}_i$, velocity $\vec{v}_i$, and angular velocity $\vec{\omega}_i$. The particles are rolling on a cylindrical, horizontal dish (radius R). We describe the system by the dimensionless dish coverage $b = N r_p^2 / R^2$; the maximum value of b is given by the condition that we only consider setups in which each particle has contact with the bottom of the dish. The dish is swirled in the horizontal plane such that each point in it has the velocity $\vec{v} = [-A\omega \sin(\omega t), A\omega \cos(\omega t), 0]$; if not stated otherwise, we consider $A = 2r_p$ and $f = \omega/2\pi = 2$ Hz. Two particles i and j only interact if the distance between their center of mass $|\vec{r}_i - \vec{r}_j|$ is smaller than $2r_p$, the overlap being $\zeta := 2r_p - |\vec{r}_i - \vec{r}_j|$. The repulsive normal force $\vec{F}_n^{(i)}$ is given by the Hertz theory with a viscoelastic dissipation [17],

$$\vec{F}_n^{(i)} = [Y\zeta^{3/2} - \gamma_n \sqrt{\zeta}(\vec{v}_i - \vec{v}_j)\vec{n}]\vec{n}, \tag{1}$$

with $\vec{n} := (\vec{r}_i - \vec{r}_j)/|\vec{r}_i - \vec{r}_j|$. We set the particle stiffness to $Y = 1.0 \times 10^5\ \mathrm{kg\,m^{-1/2}\,s^{-2}}$ and the damping constant to $\gamma_n = 30.0\ \mathrm{kg\,m^{-1/2}\,s^{-1}}$. The shear force, perpendicular to $\vec{n}$, is

*Electronic address: koetter@mpi-dortmund.mpg.de
†Electronic address: egoles@dim.uchile.cl
‡Electronic address: markus@mpi-dortmund.mpg.de

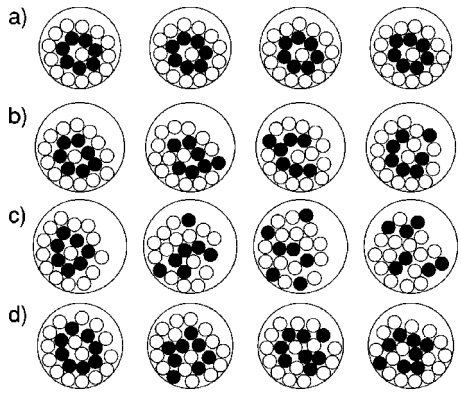

FIG. 1. Snapshots of dynamical modes taken every $\Delta t = 10 f^{-1}$ (f^{-1}: swirling period) for varying particle numbers N and dish coverages b; the dish is at 3 o'clock of its counterclockwise, horizontal swirling motion (seen from above). Some particles are marked black to visualize their displacements. (a) Shell structure with stable rings ($N=21, b=0.6$). (b) Transition mode in which particles are occasionally exchanged between rings ($N=21, b=0.5$). (c) Disordered mode for $N=21$, $b=0.45$. (d) Disordered mode for $N=23$, $b=0.6$.

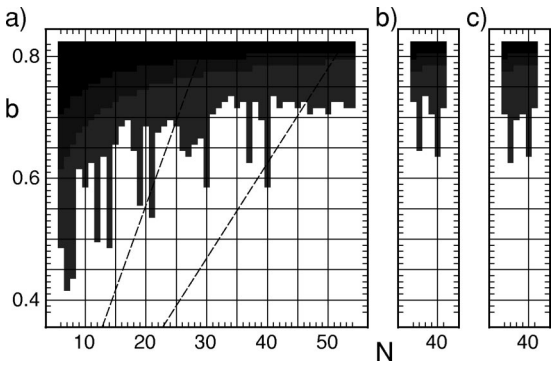

FIG. 2. System behavior depending on the dish coverage b and the number of particles N. The white region indicates disorder (fluidlike phase) or the transition mode. The dark region above indicates the solidlike phase. The particularly long dark columns indicate the formation of stable rings at the ''magic'' N. Evaluation time: $40 f^{-1}$ (f^{-1}: swirling period). The upper and lower dashed straight lines correspond to constant dish radii $R=6r_p$ and $R=8r_p$, respectively (r_p: particle radius). The driving amplitude A and frequency f of the swirling motion is varied: (a) $A=2r_p$, $f=2$ Hz, (b) $A=4r_p$, $f=1$ Hz, and (c) $A=1r_p$, $f=1$ Hz.

$$\vec{F}_s^{(i)} = -\frac{\vec{v}_s}{|\vec{v}_s|}\min\{\mu_s|\vec{F}_n^{(i)}|, \gamma_s|\vec{v}_s|\}. \tag{2}$$

The first term describes the Coulomb sliding friction and the second term a viscous friction. The shear velocity is $\vec{v}_s = \vec{v}_i - \vec{v}_j - [(\vec{v}_i - \vec{v}_j)\vec{n}]\vec{n} + r_p\vec{n}\times(\vec{\omega}_i + \vec{\omega}_j)$ and the parameters are set to $\gamma_s = 20.0$ kg s^{-1} and $\mu_s = 0.45$. Equations (1) and (2) are in good agreement with experimental observations [18]. The interaction of particle i with the boundaries (bottom and wall) of the dish were computed by assuming a particle placed symmetrically to i with respect to this boundary. In addition the rolling friction is modeled by

$$\vec{F}_r = \mu_r \frac{|F_n^{(i)}|}{r_p}\frac{\vec{v} - \vec{v}_i}{|\vec{v} - \vec{v}_i|} \tag{3}$$

with $\mu_r = 3.0\times 10^{-5}$ m; gravity is acting along the negative z axis. The differential equations are solved by a Gear-predictor-corrector algorithm [19] of sixth order with a time step of 5×10^{-5} s. This model with these parameters was optimized by fitting simulations of probability distributions, rotation frequency, and mean kinetic energy of clusters of spheres in a dish, all as functions of N, as well as single sphere trajectories to experiments performed using the setup in Ref. [16], as will be published elsewhere [20].

III. RESULTS AND DISCUSSION

The dish is swirled counterclockwise. Therefore and because of its inertia the cluster is more or less unrolling at the wall of the dish [16,20]; its center of mass is moving circularly in the dish with the same frequency as the external driving. We will focus here on the dynamics of the particles inside the cluster. We obtained three different dynamical modes, which are exemplified in Fig. 1: (a) Confinement of particles in rings (solidlike mode); (b) formation of rings that exchange particles (transition mode); and (c) and (d) disordered configurations (fluidlike mode). Solidification occurs here [compare Figs. 1(a), 1(b), and 1(c)] by increasing b. This is comparable to the well-known solidification for particle densities above a critical dilatancy [9,13]. However, we obtain here the novelty that solidification only occurs at very particular values of N, which we call ''magic numbers.'' The ring structure in Fig. 1(a) indicates that $N=21$ is such a number, while $N=23$ [Fig. 1(d), for which b is the same as in Fig. 1(a)] is not. In fact, if during calculations we add one particle in Fig. 1(a), the rings are rapidly destroyed; if we take away two particles in Fig. 1(d), rapid solidification into stable rings occurs. An overview of ring confinement versus disorder, for varying b and N, is given in Fig. 2(a). The lower, white region corresponds to disorder, while the upper, dark region corresponds to stable behavior. This dark region is connected to dark vertical bars, which are particularly long for $N=7,8,12,14,19,21,30,37,40$ (''magic numbers''). In Fig. 3 we show the ''frozen'' ring structures corresponding to these numbers. Experiments with this setup have already been performed and confirmed solidification into these structures [21].

For nonmagic N in the dark region of Fig. 2, solidification is forced by a lack of space and is not characterized by ring structures. This additional, trivial static mode is to be contrasted with the three dynamical modes described above. The ordinate of Fig. 2 ends at random loose-packing (RLP) structures, for which $b=\pi^2/12\approx 0.822$ [1]. The two curves delimiting different shadings in the upper dark region of Fig. 2 correspond to a RLP structure with a ''hole'' that could accomodate one particle (upper curve) or two particles (lower curve); these curves can be considered to indicate ''precursors'' of the fluid state and thus help to a qualitative understanding of the shape of the solidification boundary (dark-white transition) for nonmagic N.

As shown in Fig. 3, the stable configurations can be classified into four ''types'': (I) One-centered hexagonal structure, $N=1+\Sigma(6i)$; (II) one-centered ''quasicircular'' struc-

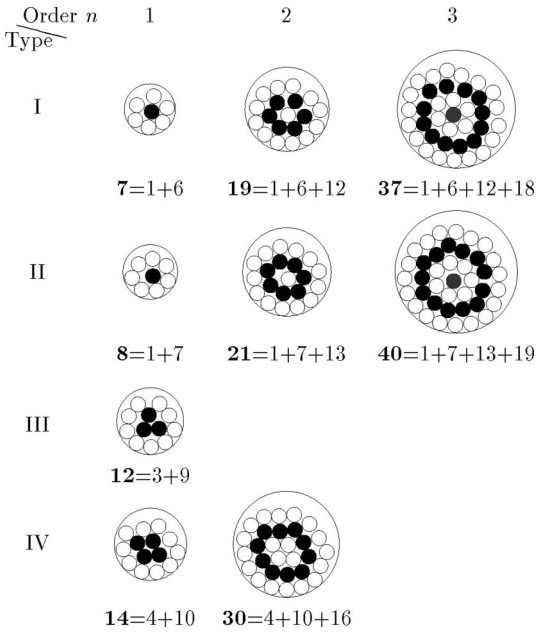

FIG. 3. ''Periodic table'' of stable shell structures. The order n (changing horizontally) is the number of rings around the center. The ''type'' (changing vertically) is related to the arrangement of particles: (I) one-centerd nearly hexagonal; (II) one-centered ''quasicircular''; (III) three centered, and (IV) four centered. The ''magic'' numbers of particles are given in bold type. The dish coverage is $b=0.6$ for $n=1$ or 2 and $b=0.63$ for $n=3$.

ture, $N=1+\Sigma(6i+1)$; (III) three particles in the center, $N=3+\Sigma(6i+3)$; and (IV) four particles in the center, $N=4+\Sigma(6i+4)$; (all sums are carried out from $i=1$ through n). No stable ring structure is found for $n\geqslant 2$ in type III (i.e., $N=27$ is not ''magic''), for $n\geqslant 3$ in type IV and for $n\geqslant 4$ in types I and II. Stable configurations can only persist if the particles have a vanishing speed relative to each other. The moving wall tends to destroy stable shell structures by accelerating the particles; the damping of the resulting velocities is maximized by a large number of contact points between particles. On the other hand, the cylindrical dish and its circular swirling motion impose circular cluster geometries. These two conditions — large number of interparticle contacts and circular motion — are optimally approximated in the stable shell structures. The sum formulas given above for types I, III, and IV are obtained by starting with one, three, or four center particles, respectively, and adding further particles in an hexagonal configuration around the center until the rings are closed. The sum formula for type II is obtained as for type I, but with a dislocation line passing nearby the center. Note that the actual structures exemplified in Fig. 3 can be understood as resulting from slight perturbations of these geometric constructions, owing to the circular motion. For the four types, an increasing number of subsequent rings leads to increasing edge lengths of the constructed geometries and thus to an increasing deviation from the externally imposed circular geometry; in that case, perturbations of the geometrical structures are so large that the rings are destroyed.

The scenario along the dashed, straight lines in Fig. 2(a) can be easily obtained in experiments [21] and occurs at an increasing number of spheres in the dish, all other parameters

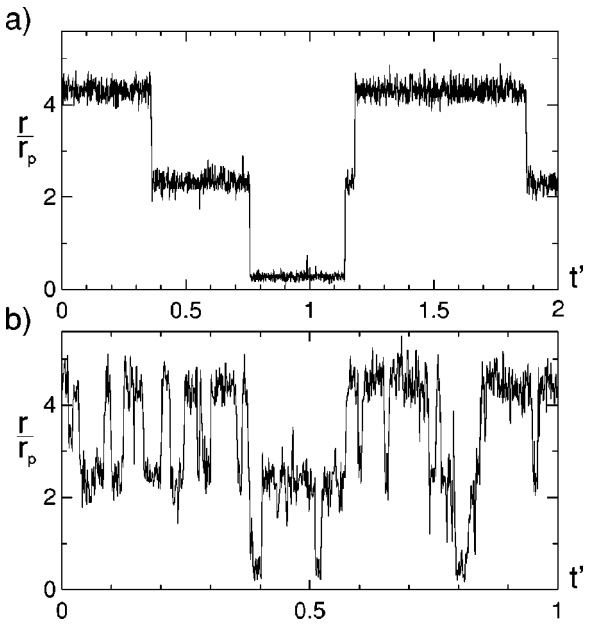

FIG. 4. Time series of the position of a single particle within the intermittent transition mode of $N=21$ particles. We plotted the distance from the center of mass of the cluster (in units of the particle radius r_p) averaged over one swirling period f^{-1} vs the dimensionless time $t'=10^{-3}$ ft. The dish coverage b is changed from (a) $b=0.51$ to (b) $b=0.44$.

being kept constant; disorder occurs above and below a singular value of N ($N=21$ for the upper straight line and $N=40$ for the lower one) at which the system ''freezes'' into rings. We found the ''magic numbers'' and their ring structures to be robust to changes of the driving amplitude A and frequency f in the following ranges: $r_p<A<4r_p$, 0.5 Hz $<f<4$ Hz [compare, for example, Figs. 2(b) and 2(c) with Fig. 2(a)]. The upper boundaries of the ranges of A and f are given by the fact that the spheres attain enough energy to move above each other for larger A and f. The lower boundaries are given by the technical constraint that computing time limits are surpassed as the system slows down for smaller A and f.

Figure 4 shows a time series of the intermittent position of

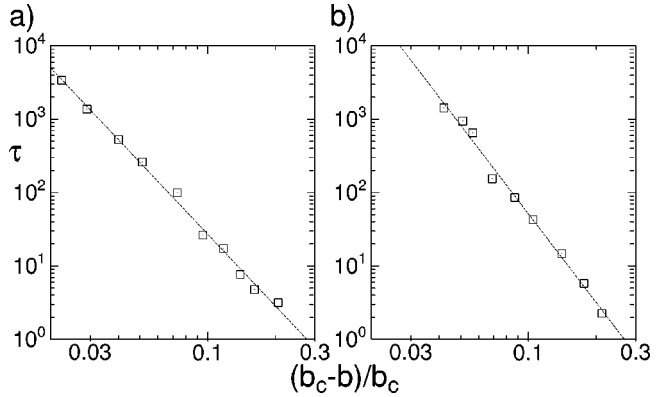

FIG. 5. The average time a particle remains in one ring (divided by the swirling period f^{-1}) vs the relative distance of b from b_c (b_c: critical value of the dish coverage b at which the stable shell structure breaks down into the transition mode). The total number of particles is (a) $N=8$ and (b) $N=21$.

a single particle within the cluster as the particle changes rings in the transition mode [see, e.g., Fig. 1(b)]. In Fig. 4(a) we see the transient lockings of the particle into each of the three rings for $N=21$, switching between the rings, as well as disordered, high frequency oscillations within each ring. In Fig. 4(b), the dish coverage b is farther away from the critical value b_c at which solidification occurs, so that switching occurs more frequently. The average time τ between switchings as a function of $|b-b_c|/b_c$ (Fig. 5) shows a dependence $\tau \propto |b-b_c|^{-\gamma}$ with $\gamma=3.25\pm0.07$, $b_c=0.45\pm0.02$ for $N=8$, and $\gamma=4.01\pm0.13$, $b_c=0.56\pm0.02$ for $N=21$. Since for an exact determination of b_c one would have to determine the solidification transition for $t\rightarrow\infty$, we determined b_c and γ in Fig. 5 by nonlinear optimization. The well-known scaling exponents for intermittency are $\gamma=1/2$ or 1 [22]. The much larger exponents found here could be an indication of crisis induced intermittency. In fact, it has been shown that for such an intermittency, higher-dimensional situations lead to enhanced values of γ; for D-dimensional maps, $(D-1)/2\leqslant\gamma\leqslant(D+1)/2$ [23]. Such an inequality is not known for continous systems; however, we do find a decrease for γ for decreasing numbers of degrees of freedom, as exemplified by the analyses of Fig. 5(a) and 5(b).

Crisis-induced intermittency in our case would mean that the fluctuations of the particles within each ring (high-frequency oscillations in Fig. 4) are described by chaotic attractors. The crisis would consist of a merging of the attractors corresponding to neighboring rings, such that both attractors touch the boundary of their basins (see [23] and references therein). In addition, it cannot be excluded that chaotic attractors correponding to the motion in the rings are defined on a manifold M that has a smaller dimension than the phase space of the whole system. In that case, switching may occur via excursions outside M, as described in Ref. [24]. The intermittency transitions found in this work are to be contrasted with granular fluid–solidlike transitions occuring via period-doubling bifurcations as reported in Refs. [15] and [25].

ACKNOWLEDGMENTS

We thank Gladys Cavallone for her dedication to arrange a fruitful stay of K. K. and M. M. in Chile, as well as the Deutsche Forschungsgemeinschaft (Grants MA 629/4) and FONDAP program in Particle Systems (Chile) for financial support.

[1] *Disordered and Granular Media*, edited by D. Bideau and A. Hansen (North-Holland, Amsterdam, 1993).
[2] *Granular Matter*, edited by A. Metha (Springer, Berlin, 1994).
[3] H.M. Jaeger, S.R. Nagel, and R.P. Behringer, Phys. Today **49**(4), 32 (1996).
[4] R.P. Behringer, Int. J. Bifurcation Chaos Appl. Sci. Eng. **7**, 963 (1997).
[5] P. Umbanhowar, F. Melo, and H.L. Swinney, Nature (London) **382**, 3838 (1996).
[6] O. Poliquen, J. Delour, and S.B. Savage, Nature (London) **386**, 816 (1997).
[7] J.B. Knight, H.M. Jaeger, and S.R. Nagel, Phys. Rev. Lett. **70**, 3728 (1993).
[8] G.H. Ristow, Europhys. Lett. **34**, 263 (1996).
[9] J.A.C. Gallas, H.J. Herrmann, and S. Sokolowski, Phys. Rev. Lett. **69**, 1371 (1992).
[10] G.H. Ristow, G. Strassburger, and I. Rehberg, Phys. Rev. Lett. **79**, 833 (1997).
[11] N. Mujica and F. Melo, Phys. Rev. Lett. **80**, 5121 (1998).
[12] Y. Zhang and C.S. Campbell, J. Fluid Mech. **237**, 541 (1992).
[13] J.A.C. Gallas, H.J. Herrmann, and S. Sokolowski, Physica A **189**, 437 (1992).
[14] H. Honda, J. Theor. Biol. **42**, 461 (1973).
[15] S. Luding, E. Clément, A. Blumen, J. Rajchenbach, and J. Duran, Phys. Rev. E **49**, 1634 (1994).
[16] M.A. Scherer, V. Buchholtz, Th. Pöschel, and I. Rehberg, Phys. Rev. E **54**, R4560 (1996).
[17] G. Kuwabara and K. Kono, Jpn. J. Appl. Phys., Part 1 **26**, 1230 (1987).
[18] J. Schäfer, S. Dippel, and D.E. Wolf, J. Phys. I **6**, 5 (1996).
[19] J. M. Haile, *Molecular Dynamics Simulation* (Wiley, New York, 1992).
[20] M. A. Scherer, K. Kötter, M. Markus, E. Goles, and I. Rehberg (unpublished).
[21] C. Krülle and I. Rehberg (private communication).
[22] H. G. Schuster, *Deterministic Chaos* (VCH, Weinheim, 1989).
[23] C. Grebogi, E. Ott, F. Romeiras, and J.A. Yorke, Phys. Rev. A **36**, 5365 (1987).
[24] J.C. Sommerer and E. Ott, Phys. Lett. A **214**, 243 (1996).
[25] F. Melo, P.B. Umbanhowar, and H.L. Swinney, Phys. Rev. Lett. **75**, 3838 (1995).